

Article

Low-Cost Fiber Rope Reinforced Polymer (FRRP) Confinement of Square Columns with Different Corner Radii

Qudeer Hussain¹, Anat Ruangrassamee^{1,*}, Somnuk Tangtermsirikul², Panuwat Joyklad³
and Anil C. Wijeyewickrema⁴

¹ Center of Excellence in Earthquake Engineering and Vibration, Department of Civil Engineering, Chulalongkorn University, Bangkok 10330, Thailand; ebbadat@hotmail.com

² School of Civil Engineering and Technology, Sirindhorn International Institute of Technology, Thammasat University, Pathum Thani 12120, Thailand; somnuk@siit.tu.ac.th

³ Department of Civil and Environmental Engineering, Srinakharinwirot University, Nakhon Nayok 26120, Thailand; panuwatj@g.swu.ac.th

⁴ Department of Civil Engineering, Tokyo Institute of Technology, Tokyo 152-8552, Japan; wijeyewickrema.a.aa@m.titech.ac.jp

* Correspondence: anat.r@chula.ac.th

Abstract: This research investigates the behavior of square concrete columns externally wrapped by low-cost and easily available fiber rope reinforced polymer (FRRP) composites. This study mainly aims to explore the axial stress-strain relationships of FRRP-confined square columns. Another objective is to assess suitable predictive models for the ultimate strength and strain of FRRP-confined square columns. A total of 60 square concrete columns were cast, strengthened, and tested under compression. The parameters were the corner radii of square columns (0, 13, and 26 mm) and different materials of FRRP composites (polyester, hemp, and cotton FRRP composites). The strength and deformability of FRRP-confined specimens were observed to be higher than the unconfined specimens. It was observed that strength gains of FRRP-confined concrete columns and corner radii were directly proportional. The accuracy of ultimate strength and strain models developed for synthetic FRRP-confined square columns was assessed using the test results of this study, showing the need for the development of improved predictive models for FRRP-confined square columns. Newly developed unified models were found to be accurate in predicting the ultimate strength and strain of FRRP-confined columns.

Keywords: square concrete columns; confinement; fiber rope reinforced polymers (FRRP); ultimate strength model; ultimate strain model; hemp fiber rope; cotton fiber rope; polyester fiber rope



Citation: Hussain, Q.; Ruangrassamee, A.; Tangtermsirikul, S.; Joyklad, P.; Wijeyewickrema, A.C. Low-Cost Fiber Rope Reinforced Polymer (FRRP) Confinement of Square Columns with Different Corner Radii. *Buildings* **2021**, *11*, 355. <https://doi.org/10.3390/buildings11080355>

Academic Editor: Jian-Guo Dai

Received: 3 July 2021

Accepted: 13 August 2021

Published: 15 August 2021

Publisher's Note: MDPI stays neutral with regard to jurisdictional claims in published maps and institutional affiliations.



Copyright: © 2021 by the authors. Licensee MDPI, Basel, Switzerland. This article is an open access article distributed under the terms and conditions of the Creative Commons Attribution (CC BY) license (<https://creativecommons.org/licenses/by/4.0/>).

1. Introduction

Earthquakes in various regions have revealed the fragile state of existing infrastructure, characterized by substandard reinforcement practices, such as weak lateral stirrup arrangements with far less confining performance and wide spacing [1–3]. Therefore, the strengthening of reinforced concrete (RC) columns in existing buildings has become essential [4]. Concrete and steel plate jacketing methods are among the pioneer practices to strengthen RC columns in existing buildings by external confinement [5,6]. The mortar or concrete jacketing method has several disadvantages; the method is labor-intensive, time-consuming, and imparts additional weight to structures, as well as occasional difficulty during in situ application [7]. Furthermore, steel jacketing could induce problems involving corrosion and handling heavy steel plates. Current synthetic fiber-reinforced polymer (FRP) composites are often used for rehabilitation, repair, and strengthening. The synthetic FRP composites are more lightweight compared with the concrete and steel jacketing. FRPs also have successfully served their purpose as an external jacketing method for concrete structures [8–10]. In the past, several types of synthetic FRP composites have

successfully been used in strengthening and retrofitting square and rectangular concrete columns [11–13]. These FRP composites are wrapped around the RC columns using epoxy or polyester resins [14,15]. The advantageous effects of FRP wrapping around the concrete surface have been studied through experimental research. Theoretical investigations have also been conducted to develop relationships for ultimate strength, axial strain, lateral dilation, and Poisson's ratio.

Rochette and Labossiere (2000) used aramid and carbon FRPs to confine square and rectangular columns [16]. The FRP composites were applied in a different number of layers in each case. The corner radii of square and rectangular columns were 5, 25, and 38 mm. They found that the section shape had a significant effect on the efficiency of FRP confinement. Rectangular concrete columns with a sharp corner radius (i.e., 5 mm) demonstrated minimal confinement effects due to FRP. Pessiki et al. (2001) used carbon and glass FRP composites to confine circular and square concrete columns [17]. The square columns were constructed with a corner radius of 38 mm. The FRP composites were developed by using unidirectional and multidirectional fabrics. The efficiency of carbon FRP composites was found to be higher than the glass FRP composites. Moreover, the shape of the concrete columns considerably affected the behavior of carbon and glass FRP-confined columns. Karam and Tabbara (2004) investigated the corner effects of square columns externally confined by carbon FRP composites [18]. They used the traditional compression test method and an innovative test method for sharp corners. The efficiency of carbon FRP composite was observed to be low as the corner radius was reduced. Mostofinejad et al. (2015) investigated the use of CFRP composites to confine the rectangular columns [19]. The rectangular columns were constructed with different corner radii: 5, 15, 25, and 38 mm. The authors reported that decreasing the corner radius reduced the ultimate strength and ductility of the CFRP confined rectangular columns. Zhu et al. (2020) conducted axial compression tests on small-scale and large-scale CFRP confined square concrete columns with or without section curvilinearization. It was found that section curvilinearization was useful to enhance the strength but had little effect on ultimate strain [20]. Han et al. 2020 studied the use of large rupture strain FRP composites to confine the square concrete columns with different corner radii from 0 to 75 mm [21]. The authors reported that as the corner radius increased, the ultimate strength of large rupture strain FRP-confined specimens also increased. Previous studies conducted on FRP-confined square and rectangular columns concluded that the axial behaviors of columns were significantly governed by corner radius [22–24].

Over the years, the effectiveness of natural and synthetic FRPs in confining the circular and non-circular columns has been extensively studied. A wide range of expressions has also been suggested by researchers for ultimate strength and strain predictions [25,26]. Shehata et al. (2002) used CFRP composites to confine circular, square, and rectangular concrete columns [27]. In their study, a corner radius of 10 mm was provided for non-circular sections. Different analytical models were proposed for each cross-section based on experimental results. Lam and Teng (2003) conducted tests on non-circular columns confined with CFRPs. A corner radius of 38 mm was provided for non-circular sections. A modified model was proposed for FRP-confined concrete using the test results and previously published database [28]. Wei and Wu (2012) later modified their previously suggested models and introduced new ones. Jiang and Nistico (2019) developed a modified local-to-global methodology to predict the stress versus strain behavior of FRP-confined square columns [29]. In another study, Shan et al. 2019 developed a modified strength model for FRP-confined square columns. They found a suitable correlation between the experimental and predicted values [30]. Boyd (2002) developed a new system, namely sprayed FRP (SFRP) composites for strengthening RC members [31]. This technique involves high-speed spraying of glass, carbon, or aramid fibers with suitable resin on the concrete surface [32,33]. In another study, Hussain et al. (2016) investigated the axial responses of square and circular columns confined with SFRP composites. A corner radius of 20 mm was provided to reduce stress concentrations at the corners. The results concluded

that the effects of SFRP composite confinement on circular columns were significantly higher than those on square columns [34].

The high material cost of fibers and epoxy resins may hinder the advantages and successful applications of FRPs [35]. A new FRP composite system, namely natural FRP, has been recently proposed as a replacement for synthetic FRP confinement [36]. The key features of natural fibers (such as sisal, hemp, and jute) include acceptable strength, high stiffness, and low density. Pimanmas et al. (2019) tested natural sisal FRP (NSFRP) confined non-circular concrete columns [37]. The strength and axial deformability of NSFRP composite confined non-circular concrete specimens were found to be higher than those of unconfined specimens. Ultimate strength and ductility were generally found to be more improved for circular columns than for square columns. Existing studies showed the effective performance of NSFRP composites in strengthening existing concrete structures [38,39].

Further investigations on a strengthening solution that could be locally available, cost-effective, and environmentally friendly without compromising its main objective of confining concrete components are still necessary. Over the years, ropes have been used for dragging and lifting purposes, depicting their remarkably high tensile strengths. Research efforts on the practice of polypropylene fibers, tapes, and un-bonded steel wires have shown that these materials are considerably useful for repair and strengthening purposes [40–42]. Hussain et al. (2020) recently developed a novel technique for strengthening concrete structures by confining them with fiber rope reinforced polymer (FRRP) composites [43]. In this technique, fiber ropes (non-impregnated) are attached to the concrete columns manually or by any suitable method with some pre-tension. Epoxy resin can be easily applied by using a roller or brush after dry wrapping. Promising advantages of FRRP composites include affordable cost and easy application. FRRP composites are also more environmentally friendly compared with synthetic CFRP, GFRP, and AFRP composites.

Previous studies on axial compressive responses of non-circular concrete columns (such as square and rectangular) externally confined with synthetic FRPs have shown that confinement is less effective than circular columns, as mentioned above. The effectiveness of FRRP confinement needs detailed investigation for non-circular concrete columns. This study investigated the axial compressive response of square concrete specimens externally confined with different types of FRRP composites. Square plain concrete specimens with different corner radii were fabricated and tested to failure under axial compression. Other studied parameters were types of FRRP composites: polyester FRRP, hemp FRRP, and cotton FRRP, as well as the number of FRRP layers. Existing predictive models for ultimate strength and strain were employed to check their accuracies for predicting the ultimate strength and strain of FRRP-confined square concrete specimens of this study. Finally, new unified models were proposed to predict the ultimate compressive strength and strain of FRRP-confined square columns.

2. Test Program

The test program comprised 60 plain square concrete specimens with three different corner radii $R_c = 0, 13, \text{ and } 26 \text{ mm}$ and various confinement levels (Figure 1). The test program is categorized into three different groups I, II, and III depending on their corner radii (Table 1). Test specimens were strengthened using hemp, cotton, and polyester fiber ropes. Furthermore, each type of rope confinement was conducted in one, two, and three layers. Hence, each group comprised a total of 20 specimens, including two control specimens.

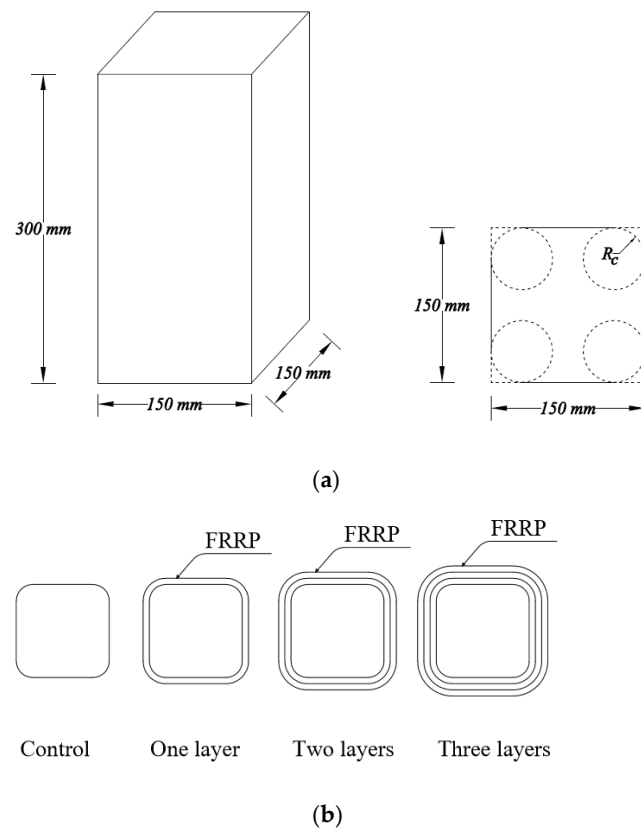


Figure 1. Details of specimens. (a) Unconfined specimen. (b) Details of FRRP confinement.

Table 1. Test program.

Group	Concrete Specimen	Corner Radius (Mm)	FRRP Type	Number of FRRP Layers	Number of Specimens
I	R0-CONT	0	-	-	2
	R0-H-1L	0	Hemp	1	2
	R0-H-2L	0	Hemp	2	2
	R0-H-3L	0	Hemp	3	2
	R0-C-1L	0	Cotton	1	2
	R0-C-2L	0	Cotton	2	2
	R0-C-3L	0	Cotton	3	2
	R0-P-1L	0	Polyester	1	2
	R0-P-2L	0	Polyester	2	2
	R0-P-3L	0	Polyester	3	2
II	R13-CONT	13	-	-	2
	R13-H-1L	13	Hemp	1	2
	R13-H-2L	13	Hemp	2	2
	R13-H-3L	13	Hemp	3	2
	R13-C-1L	13	Cotton	1	2
	R13-C-2L	13	Cotton	2	2
	R13-C-3L	13	Cotton	3	2
	R13-P-1L	13	Polyester	1	2
	R13-P-2L	13	Polyester	2	2
	R13-P-3L	13	Polyester	3	2
III	R26-CONT	26	-	-	2
	R26-H-1L	26	Hemp	1	2
	R26-H-2L	26	Hemp	2	2
	R26-H-3L	26	Hemp	3	2
	R26-C-1L	26	Cotton	1	2
	R26-C-2L	26	Cotton	2	2
	R26-C-3L	26	Cotton	3	2
	R26-P-1L	26	Polyester	1	2
	R26-P-2L	26	Polyester	2	2
	R26-P-3L	26	Polyester	3	2

3. Specimen Design and Material Properties

In the previous studies [44,45], the height to cross-sectional width ratio of square specimens was 2.0. Hence, The cross-section and height of square specimens were set to achieve a height-to-cross-section width ratio of 2.0. The research parameters covered three corner radii (0, 13, and 26 mm), three types of FRRP composites, and three thicknesses of FRRP composites (Table 1). Previous studies revealed that the effectiveness of CFRP wraps in enhancing ultimate strength was higher for short columns than slender columns [46,47]. However, a constant height was adopted for all square specimens in this study. Steel molds were made to have the required corner radii. Concrete was placed in three layers, and a vibration table was used for compaction until no further bubbles remained on the concrete surface with attention to corner zones. Another group of 18 cylinder-shaped specimens of the standard size (diameter = 150 mm and height = 300 mm) was also prepared to determine concrete strength. Concrete was prepared using Ordinary Portland cement (type 1), limestone coarse aggregate, and river sand. The mix ratio of concrete was 1:2.73:4.70 (cement:sand:aggregate) in this study. The water-to-cement ratio was 0.75. The designed 28-day compressive strength of the concrete was 20 MPa. The actual values of concrete strength during testing were 16.1, 15.4, and 14.9 MPa for hemp FRRP, cotton FRRP, and polyester FRRP-confined specimens, respectively. The strength is typical for low-rise houses. The FRRP composites were developed by using locally available hemp, cotton, and polyester fiber ropes and two-part resin (resin and hardener). The nominal diameters of hemp, cotton, and polyester fiber ropes were 2.1, 2.4, and 2.8 mm, respectively. The mix of resin corresponds to the mix proportion of 1:2 (hardener:resin). The curing time of epoxy resin was 6 to 10 h. The ultimate strain and tensile strength of epoxy resin were 2.5% and 50 MPa, respectively. Tensile tests were performed on epoxy-impregnated or epoxy-coated fiber ropes to determine the mechanical properties of epoxy-impregnated fiber ropes, as shown in Figure 2. The tensile tests were conducted following standard guidelines [48,49]. The tensile stress versus strain relationships of cotton FRRP and polyester FRRP composites were observed to be bilinear (Figure 3). However, the tensile stress versus strain response of hemp FRRP composite was linear until tensile rupture of the epoxy-impregnated hemp fiber rope (Figure 3). The ultimate strains of hemp FRRP, cotton FRRP, and polyester FRRP composites were 2.3%, 13.2%, and 16.5%, respectively, while their ultimate strengths were 177.4, 129.2, and 90.8 MPa, respectively.

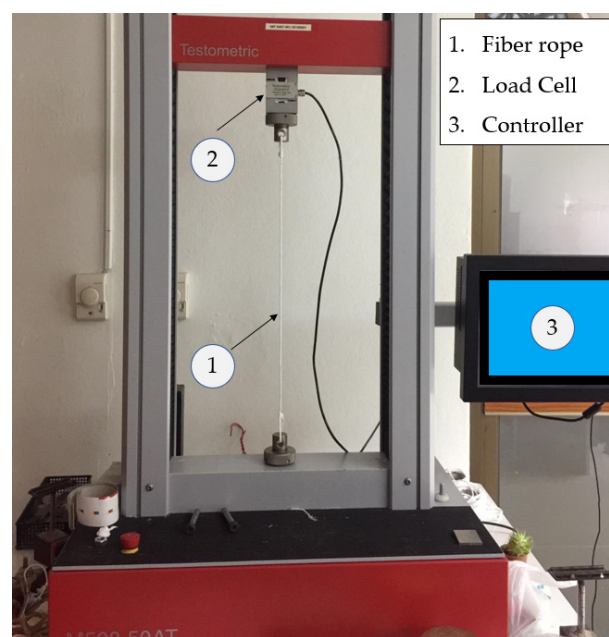


Figure 2. Setup for tensile tests.

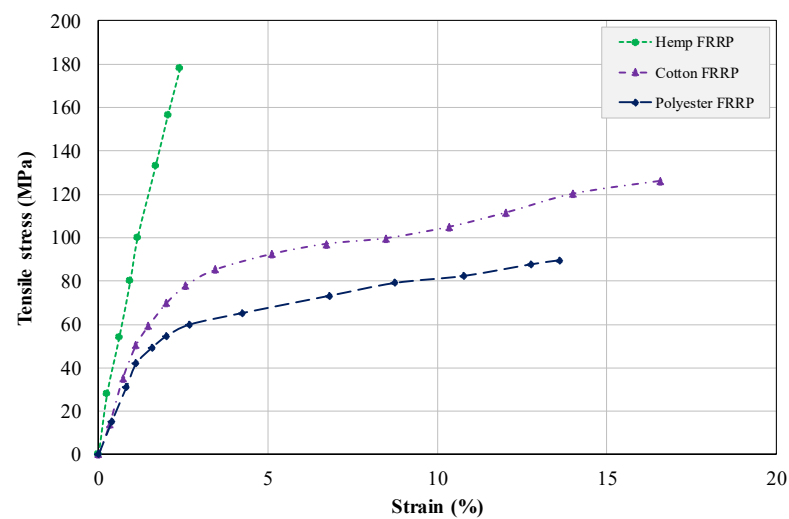


Figure 3. Tensile stress versus strain relationships of FRRP composites.

4. Strengthening of Concrete Specimens

A special mechanical system was used for dry wrapping fiber ropes circumferentially around the specimens throughout the height, as shown in Figure 4 [43]. First, dry fiber ropes were wrapped around square specimens (Figure 4b). Second, epoxy resin was applied using a brush to soak the fiber ropes completely (Figure 4c). The wrapping process ended here for specimens wrapped with a single layer of fiber ropes. For multi-layered specimens, one-layered specimens were left in a laboratory environment for 12 h before application of the second layer and another 12 h before the third layer.

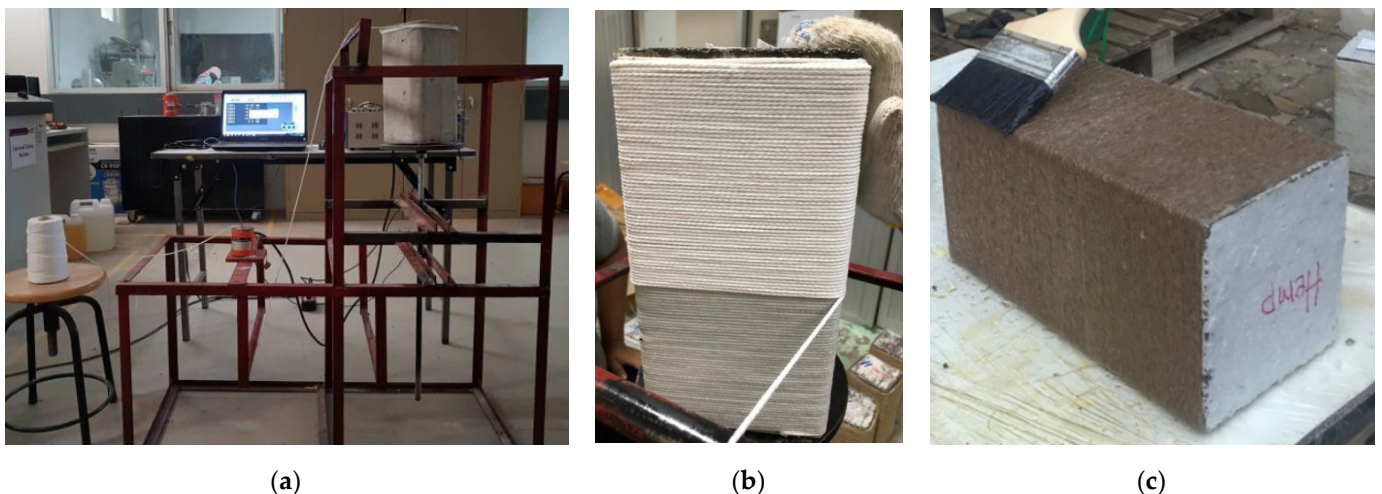


Figure 4. FRRP strengthening process (a) mechanical system (b) fiber rope wrapping (c) application of epoxy resin.

5. Instrumentation and Test Setup

Two steel frames were attached at a gauge length of 200 mm and were vertically supported by threaded rods and nuts. These vertical supports were removed before the application of the load to allow the axial deformation of specimens. Three displacement transducers were attached on three sides of the specimens to record axial deformations. Displacement transducers were mounted on the top frame, and their probes rested on another steel plate attached to the bottom frame. A universal testing machine of 2000 kN capacity was used for load application on concrete specimens. The test specimens were tested in displacement control, and an average increase in a load before the peak load was approximately 4 kN/s. Data for each specimen were recorded by a digital data logger. A

load cell with a capacity of 1000 kN was placed between the loading plate and the top of the test specimens to measure the load (Figure 5).

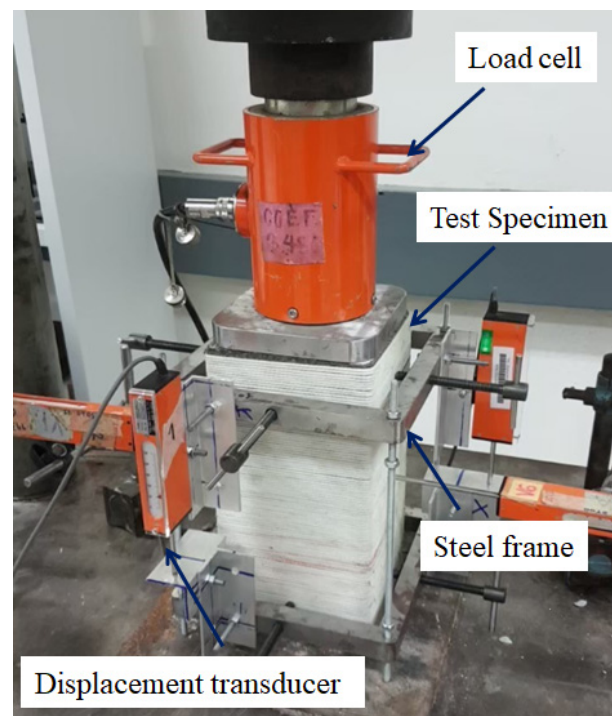


Figure 5. Typical loading setup.

6. Experimental Results and Discussions

6.1. Failure Modes of FRRP-Confined Specimens

The failures of tested specimens are shown in Figure 6. The ultimate failures of FRRP-confined specimens were mainly due to the tensile rupture of FRRP composites. Failure for specimens confined with hemp FRRP and zero corner radius was related to the tensile rupture of the FRRP jacket at the corners of square specimens (Figure 6a–c) due to the knife action. The rupture of hemp FRRP occurred at the corners of specimens regardless of the number of hemp FRRP layers. The introduction of 13 and 26 mm corner radius in square specimens shifted the rupture location of the hemp FRRP from the corners to the sides of the specimens. This failure may be caused by the flexural bending of the hemp FRRP composite under the lateral pressure from the concrete column. Since the hemp FRRP composite is brittle with a low ultimate strain, the flexure could lead to excessive local strain in the flat area in addition to the elongation normally expected from confinement. Similar failure modes were reported in other studies on FRP-confined square columns [19,20]. The rupture of hemp FRRP-confined specimens penetrated along the full height of specimens regardless of either the number of FRRP layers or corner radius (Figure 6d–f). For the 0 mm corner radius, cotton FRRP and polyester FRRP ruptured near the corners of specimens, showing a similar trend to hemp FRRP rupture. However, the introduction of the corner radius into enclosed cotton and polyester specimens did not change the location of the rupture to the sides of the specimens. In cotton FRRP and polyester, FRRP-confined specimens, severe damage of confined concrete core and excessive dilation of flat sides was observed as compared to the hemp FRRP-confined specimens. This is because the ultimate strain of cotton FRRP and polyester FRRP composites was higher than the hemp FRRP composites, as shown in Figure 3. As a result, the tensile rupture of cotton FRRP and polyester FRRP jackets was observed at the corners due to excessive dilation of flat sides and stress concentration at the corners. Li et al. 2019 also reported similar failure modes of FRP-confined square concrete columns [50]. For one and two layers of cotton FRRP and polyester FRRP-confined specimens, the rupture of FRRP composites was at the middle

(Figure 6g,h,m,n). For test specimens with three layers of cotton FRRP and polyester FRRP composites, the FRRP rupture has been mainly observed throughout the height, as shown in Figure 6i,l,o,r.



(a) R0-H-1L



(b) R0-H-2L



(c) R0-H-3L



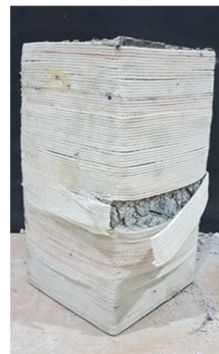
(d) R26-H-1L



(e) R26-H-2L



(f) R26-H-3L



(g) R0-C-1L



(h) R0-C-2L



(i) R0-C-3L



(j) R26-C-1L



(k) R26-C-2L



(l) R26-C-3L

Figure 6. Cont.



Figure 6. Ultimate failures of FRRP-confined specimens.

6.2. Axial Stress versus Strain Relationships

The axial stress versus strain relationships of tested specimens under uniaxial monotonic loading are shown in Figure 7. The experimental results in terms of mean values of the first peak strength (f_{fps}), stress at the maximum drop (f_{md}), ultimate strength (f_{us}), and ultimate strain (ϵ_{us}) values are summarized in Table 2. The corresponding values of gain in strength and strain are also found in Table 2. The stress versus strain curves of the hemp FRRP-confined specimens are bilinear. The first part of the curve is described by a linear part followed by a transition zone exhibiting nonlinearity accompanied by a large increase in strain. A linear stress-strain relationship is again observed in the second part but with a reduced stiffness until the sudden rupture of hemp FRRP jackets. The bilinear behavior of hemp FRRP-confined square specimens is referred to as Case-I in this study, as shown in Figure 8. In the past, the Case-1 behavior is mainly reported for the FRP-confined circular specimens, in which the confinement is provided by the uniform externally wrapped FRP composite. The Case-1 behavior was only noticed for hemp FRRP-confined square columns because of the linear stress versus strain response of hemp FRRP composites. On the other hand, the tensile stress versus strain behaviors of cotton FRRP and polyester FRRP composites were observed to be bilinear and ductile as compared to the hemp FRRP composites. As a result, a trilinear curve was observed for square concrete columns confined with cotton FRRP and polyester FRRP composites (Figure 7d–i). This trilinear curve is referred to as Case-II, as shown in Figure 8. In Case-II, the first portion is characterized by a linear line. The first portion reaches larger strength values than unconfined concrete, depending on the corner radius and confinement level. The strain at the first peak strength is denoted as ϵ_{fps} . The curve then follows a descending behavior in the second part after reaching the first peak strength. This descending behavior is an indication of inadequate confinement from cotton FRRP and polyester FRRP composites. Thus, the confined concrete significantly loses load-bearing capacity until the point of the maximum drop due to inadequate confinement. The stress at the point of the maximum

drop and corresponding strain are respectively referred to as the stress and strain at the maximum drop. The confined concrete expands laterally during the stress drop, which subsequently initiates the confinement action of the cotton FRRP and polyester FRRP composites. The third part of the stress versus strain curve is found to be linear up to the failure of the FRRP jacket. Furthermore, the Case-II response is divided into three categories, namely Case-IIA, IIB, and IIC, as shown in Figure 8, based on the potential of FRRP composite confinement and ultimate conditions compared with the unconfined specimens. In Case-IIA response, both stresses, i.e., f_{md} and f_{us} , are higher than the f_{co} . The specimens confined with FRRP composite containing Case-IIA responses are considered to be sufficiently confined specimens such as R0-C-3L and R0-P-3L (Table 2). Case-IIA responses have also been reported for FRP-confined concrete specimens [51].

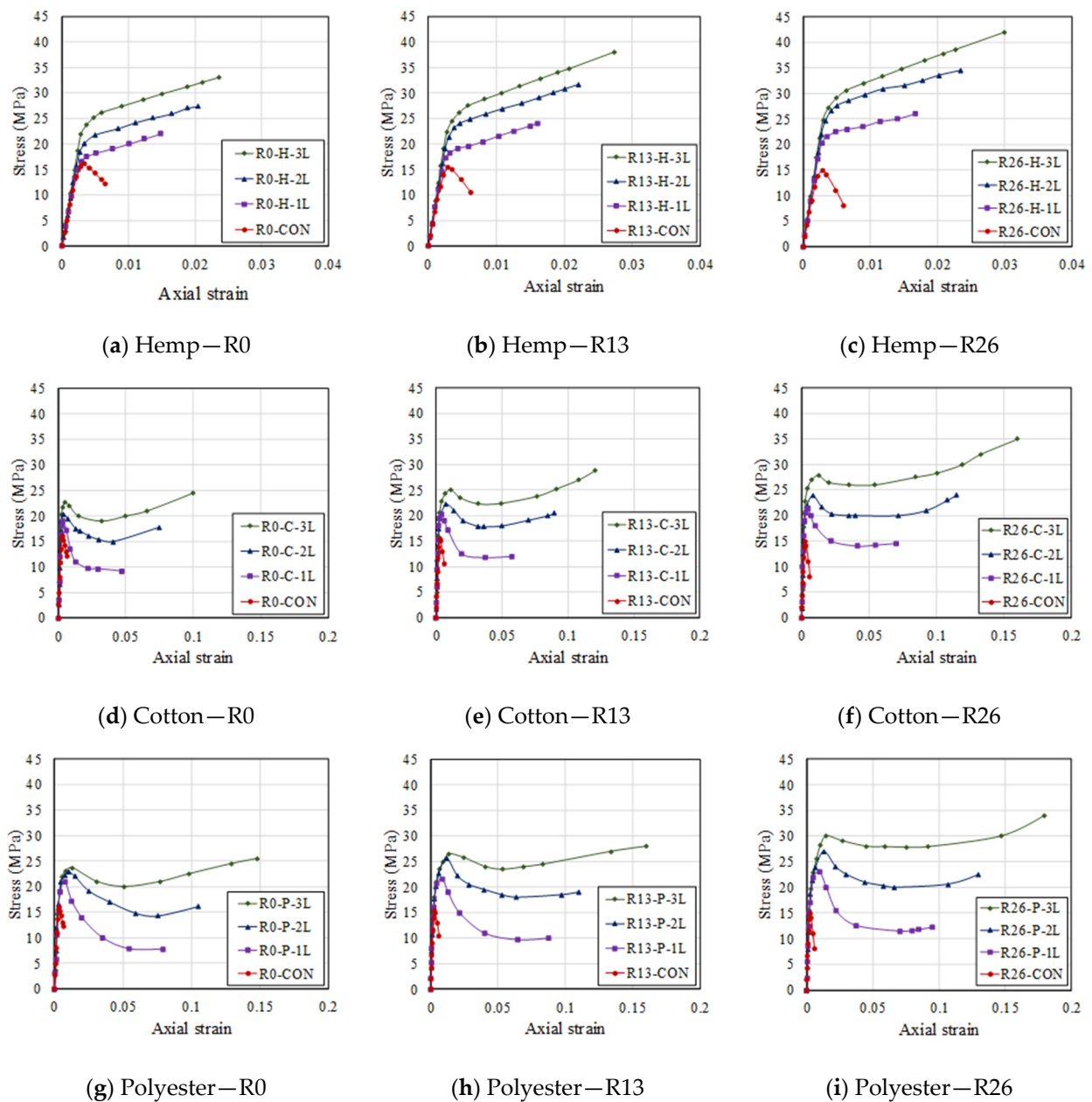


Figure 7. Stress versus axial strain curves of FRRP-confined specimens.

Table 2. Summary of experimental results.

Group	Specimen	f_{co} (MPa)	f_{fps} (MPa)	f_{md} (MPa)	f_{us} (MPa)	ϵ_{co}	ϵ_{us}	f_{fps}/f_{co}	f_{md}/f_{fps}	f_{us}/f_{co}	$\epsilon_{us}/\epsilon_{co}$	Case
I	R0-CON	16.1	-	-	-	0.0030	-	-	-	-	-	-
	R0-H-1L	16.1	-	-	22.0	0.0030	0.015	-	-	1.37	4.44	I
	R0-H-2L	16.1	-	-	27.4	0.0030	0.020	-	-	1.70	6.14	I
	R0-H-3L	16.1	-	-	33.0	0.0030	0.024	-	-	2.05	7.09	I
	R0-C-1L	16.1	19.1	9.2	9.2	0.0030	0.047	1.19	0.48	0.57	14.10	IIC
	R0-C-2L	16.1	20.3	15.0	17.8	0.0030	0.075	1.26	0.74	1.11	22.50	IIB
	R0-C-3L	16.1	22.6	19.0	24.5	0.0030	0.100	1.41	0.84	1.52	30.00	IIA
	R0-P-1L	16.1	21.0	7.8	7.8	0.0030	0.079	1.30	0.37	0.48	23.76	IIC
	R0-P-2L	16.1	22.9	14.3	16.1	0.0030	0.105	1.42	0.62	1.00	31.50	IIC
	R0-P-3L	16.1	23.7	20.0	25.5	0.0030	0.148	1.47	0.84	1.58	44.33	IIA
II	R13-CON	15.4	-	-	-	0.0029	-	-	-	-	-	-
	R13-H-1L	15.4	-	-	24.0	0.0029	0.016	-	-	1.56	5.58	I
	R13-H-2L	15.4	-	-	31.6	0.0029	0.022	-	-	2.05	7.68	I
	R13-H-3L	15.4	-	-	38.0	0.0029	0.027	-	-	2.47	9.53	I
	R13-C-1L	15.4	20.3	11.8	12.0	0.0029	0.058	1.32	0.58	0.78	20.07	IIC
	R13-C-2L	15.4	22.2	17.8	20.5	0.0029	0.090	1.44	0.80	1.33	31.41	IIA
	R13-C-3L	15.4	25.0	22.3	28.8	0.0029	0.121	1.63	0.89	1.87	42.12	IIA
	R13-P-1L	15.4	21.6	9.7	10.0	0.0029	0.088	1.40	0.45	0.65	30.54	IIC
	R13-P-2L	15.4	25.7	18.0	19.0	0.0029	0.110	1.67	0.70	1.23	38.39	IIB
	R13-P-3L	15.4	26.5	23.5	28.0	0.0029	0.160	1.72	0.89	1.82	55.84	IIA
III	R26-CON	14.9	-	-	-	0.0029	-	-	-	-	-	-
	R26-H-1L	14.9	-	-	26.0	0.0029	0.017	-	-	1.74	5.82	I
	R26-H-2L	14.9	-	-	34.5	0.0029	0.023	-	-	2.32	8.20	I
	R26-H-3L	14.9	-	-	42.0	0.0029	0.030	-	-	2.82	10.47	I
	R26-C-1L	14.9	21.4	14.0	14.5	0.0029	0.070	1.43	0.66	0.97	24.43	IIC
	R26-C-2L	14.9	23.9	20.0	24.0	0.0029	0.115	1.61	0.84	1.61	40.14	IIA
	R26-C-3L	14.9	27.8	26.0	35.0	0.0029	0.160	1.87	0.93	2.35	55.84	IIA
	R26-P-1L	14.9	23.0	11.5	12.2	0.0029	0.095	1.54	0.50	0.82	33.16	IIC
	R26-P-2L	14.9	27.0	20.0	22.5	0.0029	0.130	1.81	0.74	1.51	45.37	IIA
	R26-P-3L	14.9	30.0	27.8	34.0	0.0029	0.180	2.01	0.93	2.28	62.83	IIA

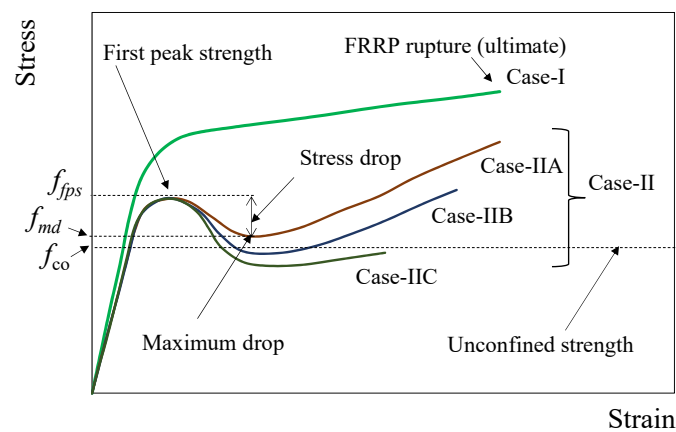


Figure 8. Typical axial stress versus strain behavior.

In some specimens, the ultimate strength f_{us} in the Case-IIB response was observed between the unconfined and first peak strength, whereas the ultimate strength in some specimens was observed higher than the unconfined strength. The FRRP-confined specimens with Case-IIB responses are regarded as specimens with moderate confinement, such as R0-C-2L and R0-P-2L (Table 2). Stress at the maximum drop and ultimate strength in the Case-IIC is lower than the unconfined strength. The specimens confined with FRRP composite with Case-IIC responses are insufficiently confined specimens such as R0-C-1L, and R0-P-1L as shown in Table 2. Case-IIC responses have also been reported for concrete confined with polymer grids and FRP-confined ultra-high-performance fiber-reinforced concrete [52,53].

6.3. Effects of FRRP Layers on Ultimate Strength and Strain

The axial stress versus strain relationships of FRRP-confined and unconfined specimens are displayed in Figure 7. Regardless of the corner radius, the stress versus strain relationships of all FRRP-confined square specimens were enhanced with the number of FRRP layers. A linear trend is found between gain in ultimate strength and the number of FRRP layers (Figure 9a). Similar to the ultimate strength, a linear trend is observed between gain in ultimate strain and confinement level, as shown in Figure 9b. Moreover, the number of FRRP layers for a specific corner radius has notable effects on first peak strength and stress drop.

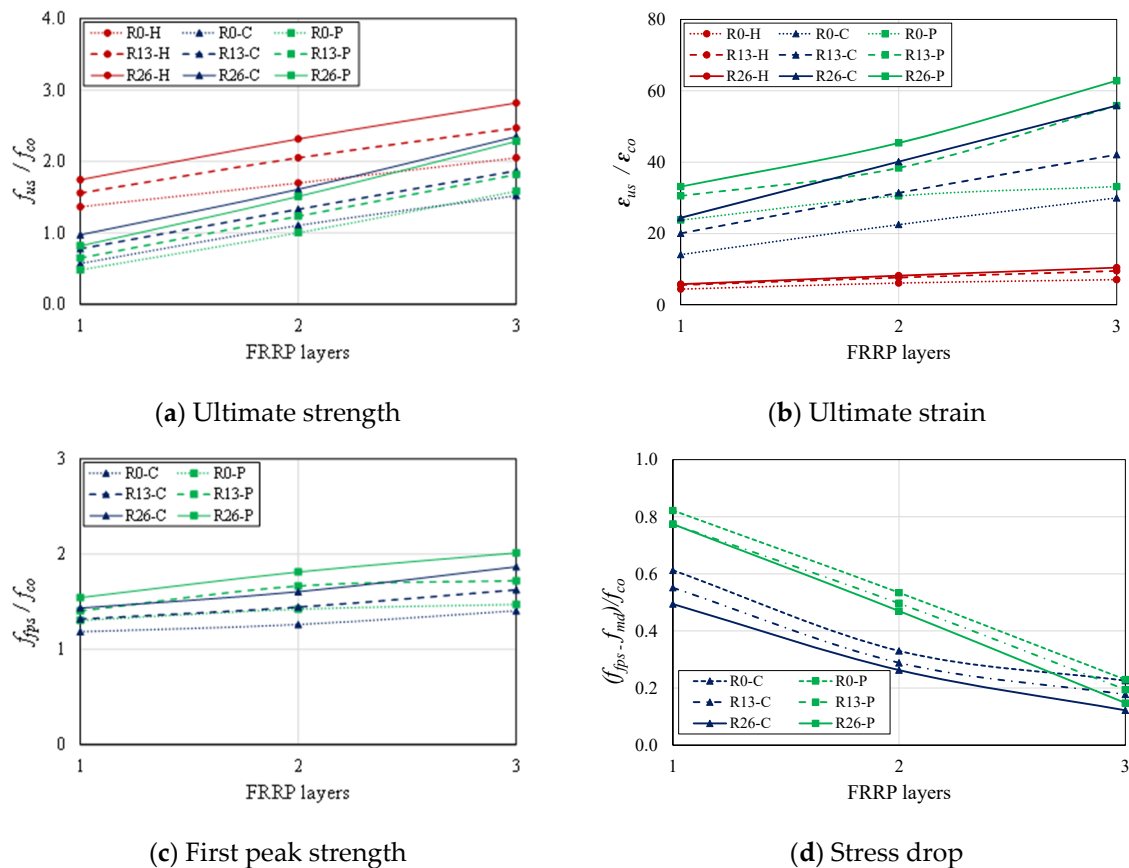


Figure 9. Effect of FRRP layers (R0 = 0 mm corner radius, R13 = 13 mm corner radius, R26 = 26 mm corner radius, H = hemp FRRP, C = cotton FRRP, P = polyester FRRP).

The first peak strength of cotton FRRP and polyester FRRP-confined specimens increases with the confinement level, whereas stress drops $(f_{fps} - f_{md})/f_{co}$ of these specimens decrease with the increase in the number of FRRP layers (Figure 9c). The responses of cotton FRRP and polyester FRRP-confined specimens with one, two, and three layers are generally observed as Case-IIC, IIB, and IIA responses, respectively. Furthermore, the stress versus strain curves indicate that the strain corresponding to the maximum stress drop decreases with the increase in confinement level. This phenomenon is an indication that the number of FRRP layers has a significant effect on effective confinement, which initiates the third ascending portion of the stress versus strain curve of FRRP-confined square specimens. This kind of behavior has also been reported in the study of PET FRP-confined square specimens [54]. Ozbakkaloglu (2013) found that the thickness of synthetic FRP composites had a negligible effect on the stress drop of synthetic FRP-confined concrete specimens [55]. However, cotton FRRP and polyester FRRP layers considerably reduce the stress drop for all FRRP-confined square specimens in this study (Figure 9d).

6.4. Effects of Corner Radius

Figure 7 and Table 2 show that rounding the corners in FRRP-confined square specimens for a particular confinement level significantly improves the ultimate strength and strain values. The improvements of ultimate strength and strain of the FRRP-confined concrete specimens with different corner radii, relative to the unconfined concrete specimens, are respectively shown in Figure 10a,b. The improvements of ultimate strength and ultimate strain of the FRRP-confined concrete specimens are directly proportional to their corner radii. These results are consistent with the conclusion drawn by Wang and Wu (2008) [45]. For the cotton FRRP and polyester FRRP-confined concrete specimens, Figure 10c,d show that the increase in the corner radius for a particular number of FRRP layers not only improves the ultimate strength but also the first peak strength (f_{fps}/f_{co}) and reduces the stress drop ($(f_{fps}-f_{md})/f_{co}$). Table 2 and Figure 10d reveal that the highest stress drop is observed for cotton FRRP and polyester FRRP-confined square specimens with no corner radius (0 mm), and the lowest stress drop is recorded for FRRP-confined square specimens with the 26 mm corner radius. Notably, corner radius provision improves the responses of the cotton FRRP, and polyester FRRP-confined specimens.

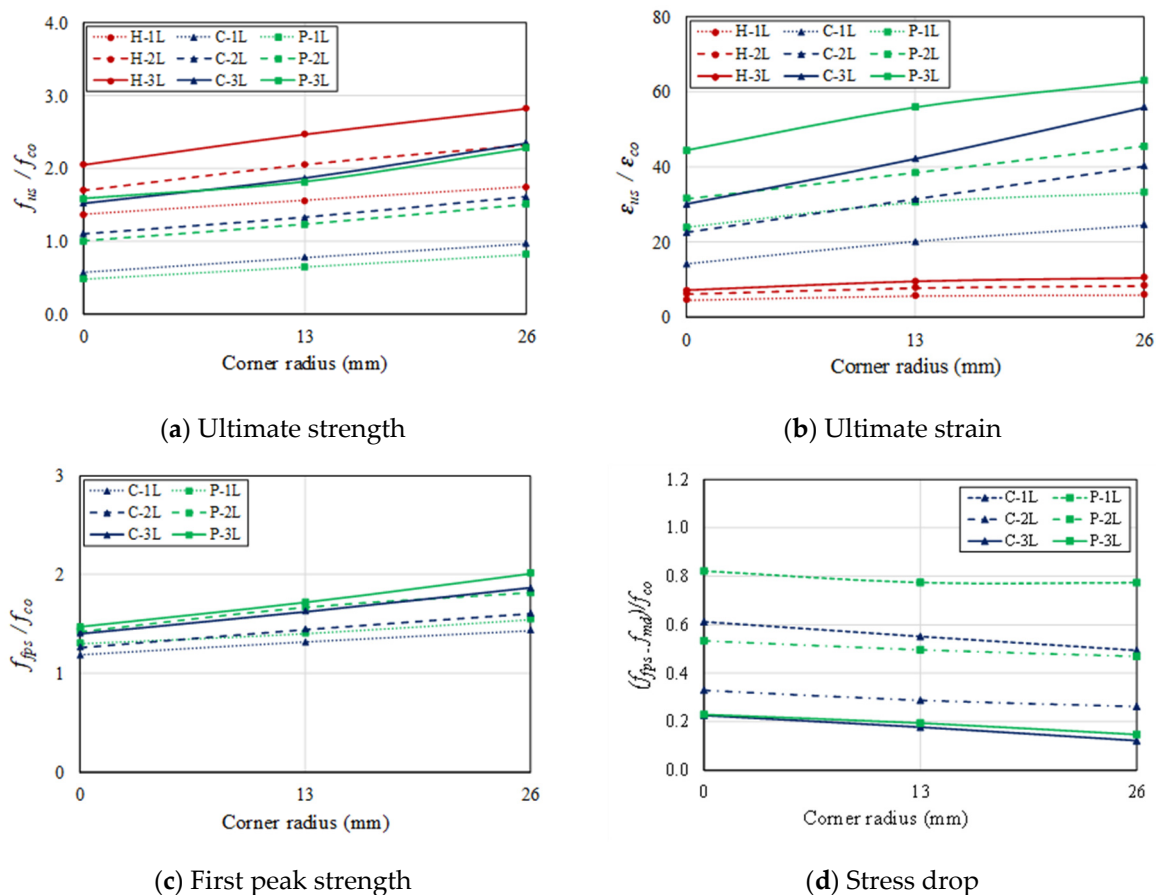
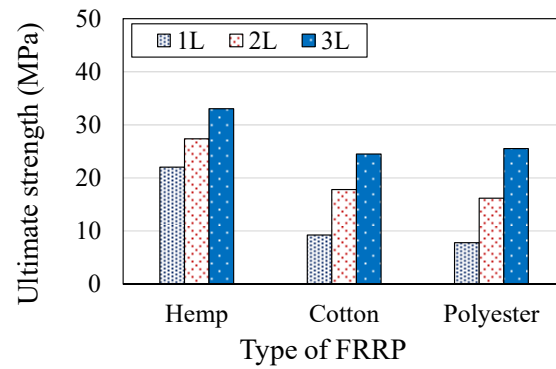


Figure 10. Effect of corner radius (H = hemp FRRP, C = cotton FRRP, P = polyester FRRP, 1L = 1 layer of FRRP, 2L = 2 layers of FRRP, 3L = 3 layers of FRRP).

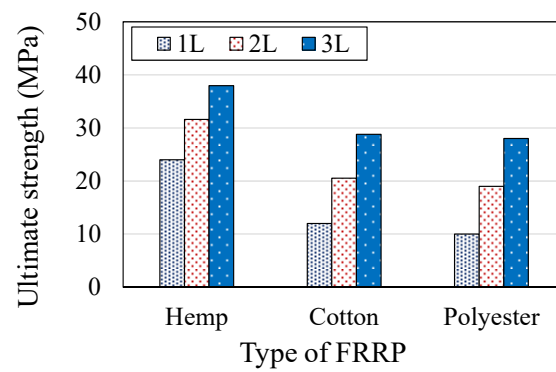
6.5. Effects of Fiber Rope Types

In Figure 7, a bilinear (Case-1) response is observed for hemp FRRP-confined square specimens. In past studies, this behavior was observed for natural and synthetic FRP-confined circular sections [43,54]. The ascending bilinear behavior of hemp FRRP-confined specimens could be related to the higher stiffness and linear stress versus strain relationships of the hemp FRRP composite, as shown in Figure 3. The axial stress versus strain responses of cotton FRRP and polyester FRRP-confined square columns are trilinear (i.e., Case-II).

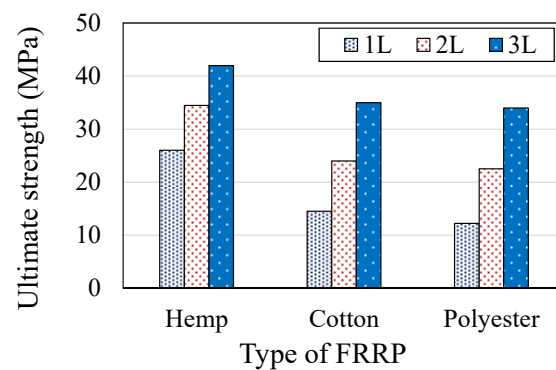
Furthermore, the comparison of ultimate strength and strain is shown in Figures 11 and 12 to investigate the comparative performance of the tested fiber rope materials. The hemp FRRP composite results in a higher ultimate strength than cotton FRRP and polyester FRRP composites, whereas the highest ultimate strain is observed for polyester FRRP-confined specimens compared with the hemp FRRP and cotton FRRP-confined specimens.



(a) Corner radius 0 mm

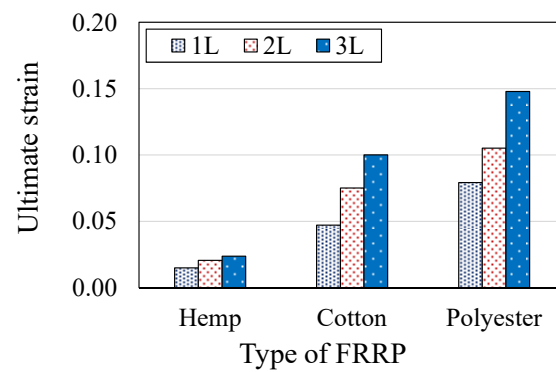


(b) Corner radius 13 mm

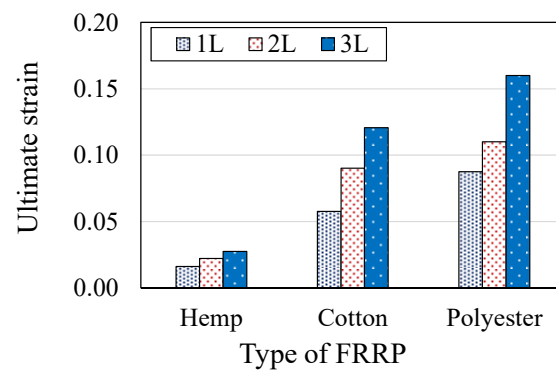


(c) Corner radius 26 mm

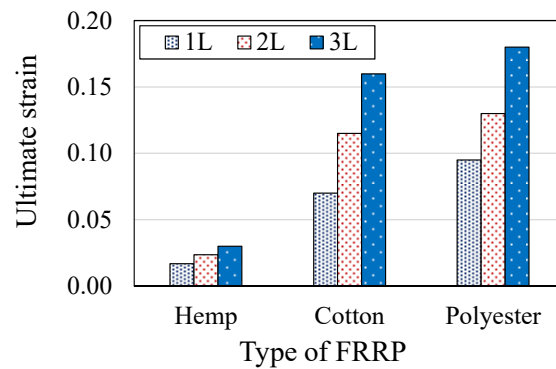
Figure 11. Effects of fiber ropes on ultimate strength (1L = 1 layer of FRRP, 2L = 2 layers of FRRP, 3L = 3 layers of FRRP).



(a) Corner radius 0 mm



(b) Corner radius 13 mm



(c) Corner radius 26 mm

Figure 12. Effects of fiber ropes on ultimate strain (1L = 1 layer of FRRP, 2L = 2 layers of FRRP, 3L = 3 layers of FRRP).

7. Strength and Strain Models

7.1. Compressive Strength Models

Previous studies have proposed different expressions for predicting the ultimate compressive strength of the circular and square plain concrete specimens externally confined with FRPs [27,37]. The ultimate strength (f_{us}) of FRP-confined concrete is associated with the unconfined strength (f_{co}) of concrete in the following form.

$$\frac{f_{us}}{f_{co}} = 1 + k_1 \cdot \rho \left(\frac{f_{cp}}{f_{co}} \right) \quad (1)$$

where f_{cp} represents lateral pressure due to FRP in the hoop direction, k_1 represents the coefficient of FRP confinement, and ρ is the shape factor. In the past, different ultimate

strength models have been proposed, especially for FRP-confined concrete, by employing Equation (1) with the modified expression for the confinement effectiveness coefficient k_1 [56]. The majority of these models described k_1 in a nonlinear form considering f_{ts}/f_{co} or f_{cp} , where f_{ts} is the tensile strength of FRP. A linear trend between ultimate strength and the lateral confining pressure was observed in the previous studies. Following this linear trend, constant values of k_1 were suggested in those studies for different types of FRPs. The lateral confining pressure f_{cp} was often related to the tensile strength (f_{ts}) [35,37,44] or hoop rupture strain [57]. For the design purpose, the tensile strength is the straightforward and widely accepted parameter in the application. The lateral confining pressure f_{cp} is related to the confinement level, that is, the number of FRP layers (t) and tensile strength (f_{ts}) of the FRP in the following form:

$$f_{cp} = \frac{2f_{ts}t}{D} \quad (2)$$

where D represents the diagonal length of the non-circular sections (Figure 13) and diagonal length D in the case of the non-circular section with rounded corners can be calculated by using the following relationship:

$$D = \frac{2wd}{w+d} \quad (3)$$

where d and w represent the depth and width of non-circular sections, respectively (Figure 13). ρ in Equation (1) is a shape factor defined by ACI-440.2 R-02 [58] in the following form:

$$\rho = 1 - \frac{(w - 2R_c)^2 + (d - 2R_c)^2}{3A} \quad (4)$$

where R_c is the corner radius, and A represents the gross area of the core concrete.

$$A = wd - (4 - \pi)R_c^2 \quad (5)$$

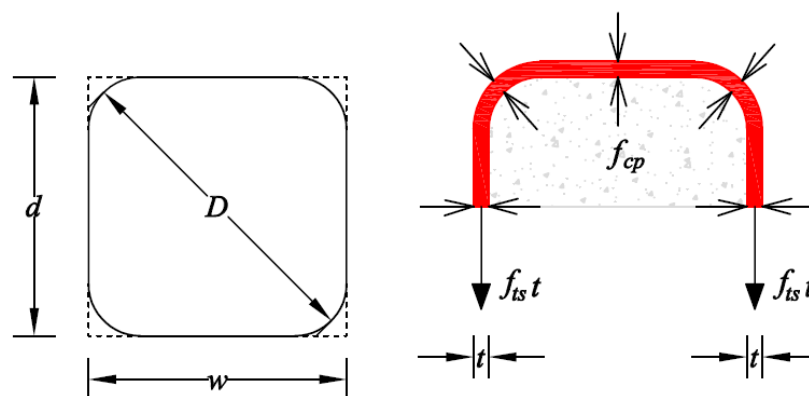


Figure 13. FRP confinement of square sections.

7.2. Ultimate Strain Models

Previous research results showed that the ultimate strain ε_{us} corresponding to the ultimate compressive strain for concrete confined with steel reinforcement could be related to the lateral confining pressure in the following form:

$$\frac{\varepsilon_{us}}{\varepsilon_{co}} = 1 + k_2 \left(\frac{f_{cp}}{f_{co}} \right) \quad (6)$$

where ε_{us} is the ultimate axial strain of concrete and k_2 is the strain enhancement coefficient. Richart et al. (1928) proposed $k_2 = 5k_1$, for concrete confined with steel reinforcement [56]. Furthermore, Fardis et al. (1981) proposed a relationship between the ultimate strain (ε_{us}) of the FRP-confined concrete and lateral confining pressure (f_{cp}) [59]. Some existing

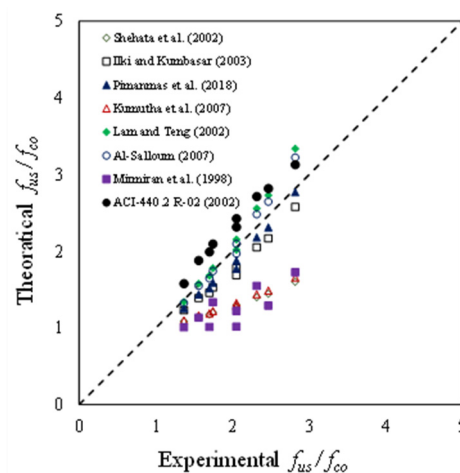
expressions of ultimate strength and strain for FRP-confined square columns are listed in Table 3.

Table 3. Strength and strain models.

Researcher	Ultimate Strength Model	Ultimate Strain Model
Shehata et al. (2002) [27]	$\frac{f_{us}}{f_{co}} = 1 + 0.85 \left(\frac{f_{cp}}{f_{co}} \right)$	$\frac{\epsilon_{us}}{\epsilon_{co}} = 1 + 0.85 \left(\frac{f_{cp}}{f_{co}} \right)$
Ilki and Kumbasar (2003) [60]	$\frac{f_{us}}{f_{co}} = 1 + 2.227 \left(\frac{f_{cp}}{f_{co}} \right)$	$\frac{\epsilon_{us}}{\epsilon_{co}} = 1 + 15 \left(\frac{f_{cp}}{f_{co}} \right)^{0.75}$
Pimanmas et al. (2019) [37]	$\frac{f_{us}}{f_{co}} = 1 + 2.50 \left(\frac{f_{cp}}{f_{co}} \right)$	$\frac{\epsilon_{us}}{\epsilon_{co}} = 2 + 7.0 \left(\frac{f_{cp}}{f_{co}} \right)$
Kumutha et al. (2007) [61]	$\frac{f_{us}}{f_{co}} = 1 + 0.93 \left(\frac{f_{cp}}{f_{co}} \right)$	-
Lam and Teng (2002) [62]	$\frac{f_{us}}{f_{co}} = 1 + 3.30 \left(\frac{f_{cp}}{f_{co}} \right)$	$\frac{\epsilon_{us}}{\epsilon_{co}} = 1.75 + 12 \left(\frac{f_{cp}}{f_{co}} \right) \left(\frac{\epsilon_{fe}}{\epsilon_{co}} \right)^{0.45}$
Al-Salloum (2007) [44]	$\frac{f_{us}}{f_{co}} = 1 + 3.14 \left(\frac{b}{D} \right) \left(\frac{f_{cp}}{f_{co}} \right)$	-
Mirmiran et al. (1998) [63]	$\frac{f_{us}}{f_{co}} = 1 + 6.0 \left(\frac{2r}{D} \right) \left(\frac{f_{cp}}{f_{co}} \right)^{0.70}$	-
ACI-440.2 R-02 (2002) [58]	$\frac{f_{us}}{f_{co}} = -1.2541 + 2.254 \sqrt{1 + \left(\frac{7.94 f_{cp}}{f_{co}} \right)} - 2 \left(\frac{f_{cp}}{f_{co}} \right)$	$\frac{\epsilon_{us}}{\epsilon_{co}} = 1.50 + 13 \left(\frac{f_{cp}}{f_{co}} \right) \left(\frac{\epsilon_{fe}}{\epsilon_{co}} \right)^{0.45}$

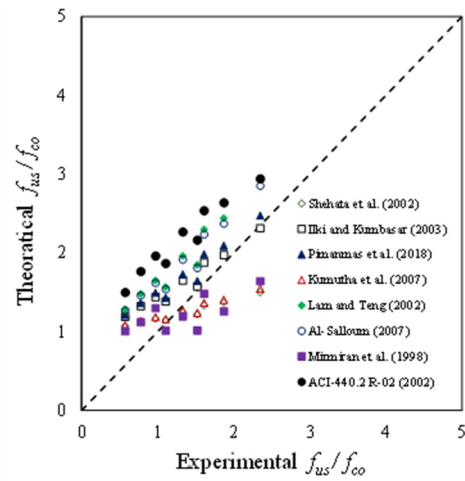
7.3. Assessment of Existing Strength and Strain Models

The applicability of existing strength and strain models listed in Table 3, which were developed for FRP-confined square specimens, on FRRP-confined specimens were assessed by comparison with the experimental results from this study. The correlations between experimental and calculated strength gain ratios (f_{us}/f_{co}) are shown in Figure 14, and those between experimental and calculated strain improvement ratios ($\epsilon_{us}/\epsilon_{co}$) are shown in Figure 15. For the strength models, only the ACI model [58] effectively fits the experimental results of the hemp FRRP-confined specimens despite higher predictions than the test results (Figure 14a). However, the model that can predict the ultimate strength of cotton FRRP and polyester FRRP-confined specimens is unavailable (Figure 14b,c). In the case of ultimate strain models, Figure 15 shows that the predictions by all models are inaccurate, except for that of Ilki and Kumbasar (2003), which is acceptable for predicting the ultimate strain of hemp FRRP-confined specimens.

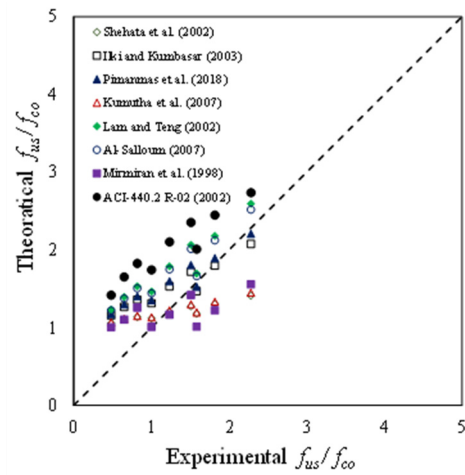


(a) Hemp FRRP specimens

Figure 14. Cont.

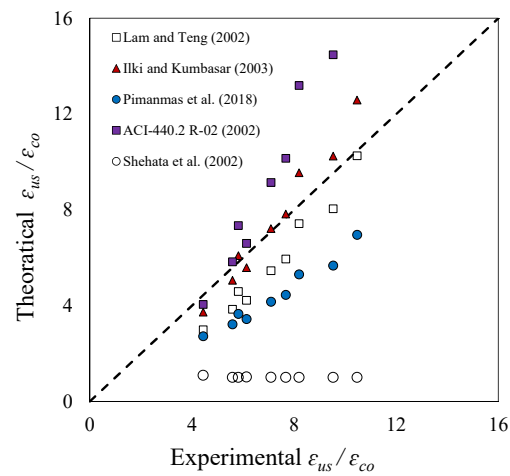


(b) Cotton FRRP specimens



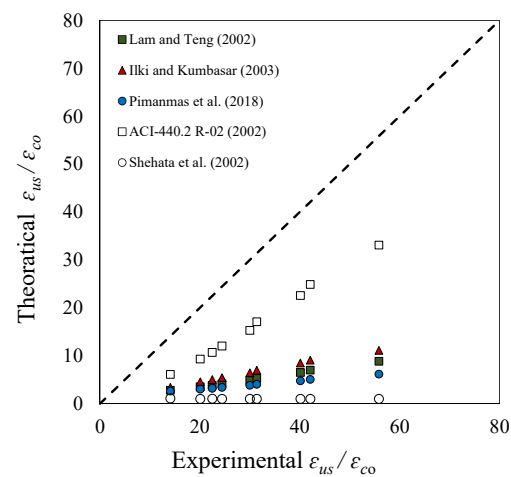
(c) Polyester FRRP specimens

Figure 14. Assessment of strength models.

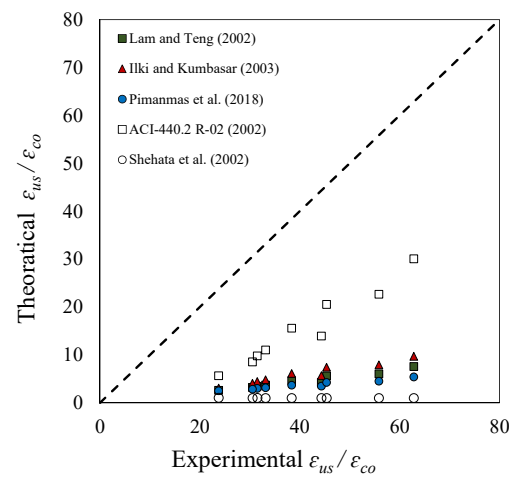


(a) Hemp FRRP specimens

Figure 15. Cont.



(b) Cotton FRRP specimens



(c) Polyester FRRP specimens

Figure 15. Assessment of strain models.

7.4. Proposed Ultimate Strength Models

New unified ultimate strength models that can be used for both FRRP-confined circular and square columns were developed by modifying the previously proposed ultimate strength models for FRRP-confined circular specimens. The test results of the current and previous studies by Wang and Wu (2008) [64] and Saleem et al. (2017) [54] showed that the strength gain (f_{us}/f_{co}) of FRP-confined specimens was proportional to the corner radius.

Wu and Wang (2009) [59] reported factors that affected the strength gain (f_{us}/f_{co}) of FRP-confined square specimens. The strength gain (f_{us}/f_{co}) of FRP-confined square specimens can be obtained by adopting a similar equation to the strength models of circular specimens as follows:

$$\frac{f_{us}}{f_{co}} = 1 + k_1 \cdot \rho^\alpha \left(\frac{f_{cp}}{f_{co}} \right) \quad (7)$$

where ρ can be determined by using Equation (4), and the constant α can be derived from a regression analysis of test results. Notably, when ρ is equal to 1, Equation (7) becomes the equation for FRRP-confined circular specimens.

The ultimate strength model proposed by Hussain et al. (2020) [38] for FRRP-confined circular specimens can be modified by applying a similar concept to predict the ultimate strength of square specimens as follows:

$$\frac{f_{us}}{f_{co}} = 1 + 2.70 \cdot \rho^\alpha \left(\frac{f_{cp}}{f_{co}} \right) \quad (8)$$

The constant α can be determined from the regression analysis of the experimental results. The following new models are then proposed for FRRP-confined square concrete specimens with different corner radii.

For hemp FRRP-confined square specimens

$$\frac{f_{us}}{f_{co}} = 1 + 2.70 \cdot \rho^{0.90} \left(\frac{f_{cp}}{f_{co}} \right) \quad (9)$$

For cotton FRRP and polyester FRRP-confined square specimens

$$\frac{f_{us}}{f_{co}} = 1 + 2.70 \cdot \rho^{1.75} \left(\frac{f_{cp}}{f_{co}} \right) \quad (10)$$

The lateral confining pressure f_{cp} can be obtained from Equation (2). The relationship between the predictions using Equations (9) and (10) and the experimental results is shown in Figure 16a. Thus, the proposed models are accurate in predicting the ultimate strength of the tested specimens.

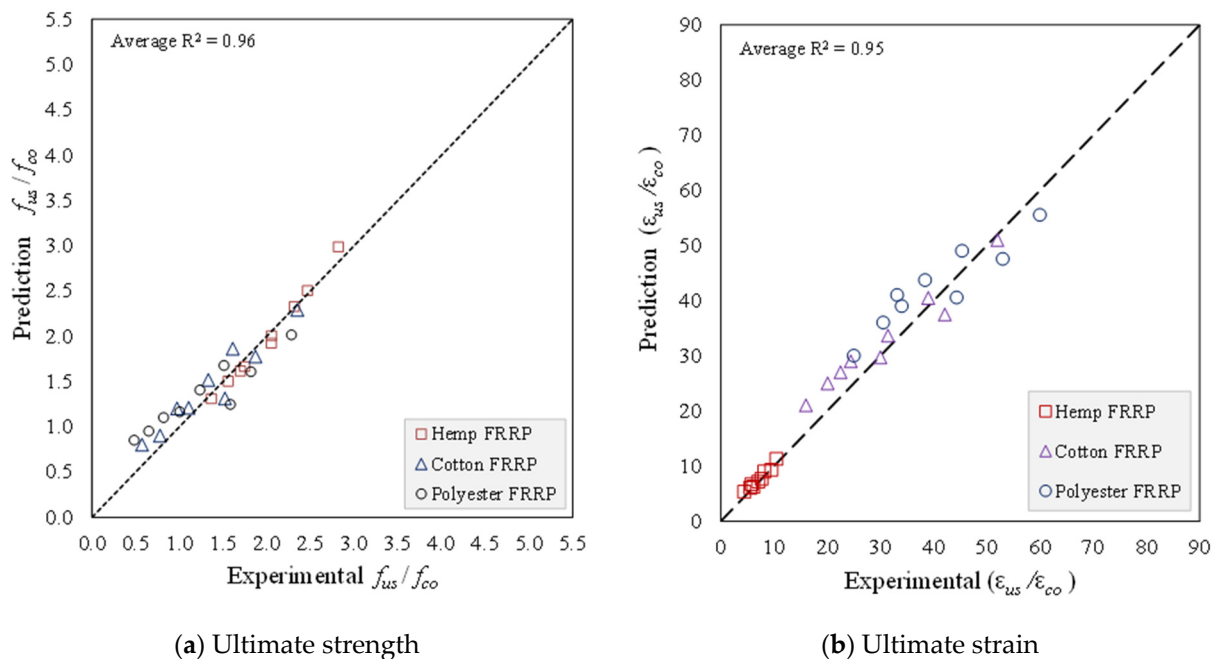


Figure 16. Verification of the proposed models.

7.5. Proposed Ultimate Strain Models

The ultimate strain models proposed by Hussain et al. (2020) [38] for the ultimate strain prediction of FRRP-confined circular specimens are modified in Equations (11)–(13) to predict the ultimate strain of FRRP-confined square specimens.

For hemp FRRP-confined square specimens

$$\frac{\epsilon_{us}}{\epsilon_{co}} = 2 + 10 \cdot \rho^{1.10} \left(\frac{f_{cp}}{f_{co}} \right) \quad (11)$$

For cotton FRRP-confined square specimens

$$\frac{\varepsilon_{us}}{\varepsilon_{co}} = 26 + 53 \cdot \rho^{2.20} \left(\frac{f_{cp}}{f_{co}} \right) \quad (12)$$

For polyester FRRP-confined square specimens

$$\frac{\varepsilon_{us}}{\varepsilon_{co}} = 34 + 53 \cdot \rho^{1.80} \left(\frac{f_{cp}}{f_{co}} \right) \quad (13)$$

The lateral confining pressure f_{cp} can be obtained from Equation (2). The relationship between the predictions using Equations (11)–(13) and the experimental results is shown in Figure 16b. It can be seen that the proposed ultimate strain models are fairly accurate in predicting the ultimate strain of the FRRP-confined square specimens with different corner radii.

8. Conclusions

A series of tests were conducted on 60 square concrete specimens with different corner radii to explore the axial stress-strain relationships in compression. The following conclusions can be drawn from experimental and analytical investigations.

1. FRRP composites are effective in enhancing the strength and deformability of confined concrete. Compressive strength and deformability for concrete specimens with a certain corner radius increase with the number of FRRP layers.
2. The corner radius had a significant effect on the behavior of FRRP-confined specimens. The ultimate strength and strain of FRPP confined concrete increased with the corner radius.
3. Experimental results demonstrate a nearly linear relationship between the strength gains of FRRP-confined square concrete specimens and corner radius.
4. Previously developed models to estimate the ultimate strength and strain of FRP-confined square columns are found incapable of precisely estimating the ultimate strength and strain of the FRRP-confined square specimens of this study. Newly developed unified models are accurate in estimating the ultimate strength and strain of FRRP-confined square columns.

Author Contributions: Conceptualization, Q.H., A.R. and S.T.; methodology, Q.H., A.R. and S.T.; validation, A.R., S.T. and A.C.W.; writing—original draft preparation, Q.H., A.R., S.T., P.J. and A.C.W.; writing—review and editing, Q.H., A.R., S.T., P.J. and A.C.W. All authors have read and agreed to the published version of the manuscript.

Funding: This research project was supported by the Second Century Fund (C2F), Chulalongkorn University and Thammasat University Research Fund under the TU research Scholar, Contract No. TP 2/28/2018.

Institutional Review Board Statement: Not applicable.

Informed Consent Statement: Not applicable.

Data Availability Statement: The data presented in this study are available on request from the corresponding author.

Acknowledgments: This research project was supported by the Second Century Fund (C2F), Chulalongkorn University. The research was also supported by the Center of Excellence in Material Science, Construction and Maintenance Technology, Thammasat University, and Thammasat University Research Fund under the TU research Scholar, Contract No. TP 2/28/2018. Thanks are also extended to Asian Institute of Technology (AIT), Thailand, for supporting test facilities.

Conflicts of Interest: The authors declare no conflict of interest.

References

1. Tastani, S.P.; Pantazopoulou, S.J. Experimental evaluation of FRP jackets in upgrading RC corroded columns with substandard detailing. *Eng. Struct.* **2004**, *26*, 817–829. [\[CrossRef\]](#)
2. Cardone, D.; Flora, A.; Picione, M.D.L.; Martocchia, A. Estimating direct and indirect losses due to earthquake damage in residential RC buildings. *Soil Dyn. Earthq. Eng.* **2019**, *126*, 105801. [\[CrossRef\]](#)
3. Sezen, H.; Lodhi, M.S. Seismic Response of Reinforced Concrete Columns. In *Earthquake-Resistant Structures: Design, Assessment and Rehabilitation*; BoD—Books on Demand: Norderstedt, Germany, 2012.
4. Hadi, M.N.; Pham, T.M.; Lei, X. New method of strengthening reinforced concrete square columns by circularizing and wrapping with fiber-reinforced polymer or steel straps. *J. Compos. Constr.* **2013**, *17*, 229–238. [\[CrossRef\]](#)
5. Tsonos, A.D. Performance enhancement of R/C building columns and beam–column joints through shotcrete jacketing. *Eng. Struct.* **2010**, *32*, 726–740. [\[CrossRef\]](#)
6. Rodriguez, M.; Park, R. Repair and strengthening of reinforced concrete buildings for seismic resistance. *Earthq. Spectra* **1991**, *7*, 439–459. [\[CrossRef\]](#)
7. Naji, A.J.; Al-Jelawy, H.M.; Saadoon, S.A.; Ejel, A.T. Rehabilitation and strengthening techniques for reinforced concrete columns. *J. Phys. Conf. Ser.* **2021**, *1895*, 012049. [\[CrossRef\]](#)
8. Ozbakkaloglu, T.; Lim, J.C.; Vincent, T. FRP-confined concrete in circular sections: Review and assessment of stress–strain models. *Eng. Struct.* **2013**, *49*, 1068–1088. [\[CrossRef\]](#)
9. Rodsin, K.; Hussain, Q.; Suparp, S.; Nawaz, A. Compressive behavior of extremely low strength concrete confined with low-cost glass FRP composites. *Case Stud. Constr. Mater.* **2020**, *13*, e00452. [\[CrossRef\]](#)
10. Karbhari, V.M.; Gao, Y. Composite jacketed concrete under uniaxial compression—Verification of simple design equations. *J. Mater. Civ. Eng.* **1997**, *9*, 185–193. [\[CrossRef\]](#)
11. Chaayasarn, K.; Hussain, Q.; Joyklad, P.; Rodsin, K. New hybrid basalt/E-glass FRP jacketing for enhanced confinement of recycled aggregate concrete with clay brick aggregate. *Case Stud. Constr. Mater.* **2021**, *14*, e00507.
12. Avossa, A.M.; Picozzi, V.; Ricciardelli, F. Load-Carrying Capacity of Compressed Wall-Like RC Columns Strengthened with FRP. *Buildings* **2021**, *11*, 285. [\[CrossRef\]](#)
13. Li, X.; Lu, J.; Ding, D.D.; Wang, W. Axial strength of FRP-confined rectangular RC columns with different cross-sectional aspect ratios. *Mag. Concr. Res.* **2017**, *69*, 1011–1026. [\[CrossRef\]](#)
14. Mufti, A.A. FRPs and FOSs lead to innovation in Canadian civil engineering structures. *Constr. Build. Mater.* **2003**, *17*, 379–387. [\[CrossRef\]](#)
15. Montoya, E.; Vecchio, F.J.; Sheikh, S.A. Numerical evaluation of the behaviour of steel-and FRP-confined concrete columns using compression field modelling. *Eng. Struct.* **2004**, *26*, 1535–1545. [\[CrossRef\]](#)
16. Rochette, P.; Labossiere, P. Axial testing of rectangular column models confined with composites. *J. Compos. Constr.* **2000**, *4*, 129–136. [\[CrossRef\]](#)
17. Pessiki, S.; Harries, K.A.; Kestner, J.T.; Sause, R.; Ricles, J.M. Axial behavior of reinforced concrete columns confined with FRP jackets. *J. Compos. Constr.* **2001**, *5*, 237–245. [\[CrossRef\]](#)
18. Karam, G.; Tabbara, M. Corner effects in CFRP-wrapped square columns. *Mag. Concr. Res.* **2004**, *56*, 461–464. [\[CrossRef\]](#)
19. Mostofinejad, D.; Moshiri, N.; Mortazavi, N. Effect of corner radius and aspect ratio on compressive behavior of rectangular concrete columns confined with CFRP. *Mater. Struct.* **2015**, *48*, 107–122. [\[CrossRef\]](#)
20. Zhu, J.Y.; Lin, G.; Teng, J.G.; Chan, T.M.; Zeng, J.J.; Li, L.J. FRP-confined square concrete columns with section curvilinearization under axial compression. *J. Compos. Constr.* **2020**, *24*, 04020004. [\[CrossRef\]](#)
21. Han, Q.; Yuan, W.; Bai, Y.; Du, X. Compressive behavior of large rupture strain (LRS) FRP-confined square concrete columns: Experimental study and model evaluation. *Mater. Struct.* **2020**, *53*, 1–20. [\[CrossRef\]](#)
22. Mukherjee, A.; Boothby, T.E.; Bakis, C.E.; Joshi, M.V.; Maitra, S.R. Mechanical behavior of fiber-reinforced polymer-wrapped concrete columns—Complicating effects. *J. Compos. Constr.* **2004**, *8*, 97–103. [\[CrossRef\]](#)
23. Zou, Y.; Hong, H.P. Reliability assessment of FRP-confined concrete columns designed for buildings. *Struct. Infrastruct. Eng.* **2011**, *7*, 243–258. [\[CrossRef\]](#)
24. Mai, A.D.; Sheikh, M.N.; Hadi, M.N. Performance evaluation of intermittently CFRP wrapped square and circularised square reinforced concrete columns under different loading conditions. *Struct. Infrastruct. Eng.* **2019**, *15*, 696–710. [\[CrossRef\]](#)
25. Algburi, A.H.; Sheikh, M.N.; Hadi, M.N. New technique for strengthening square-reinforced concrete columns by the circularisation with reactive powder concrete and wrapping with fibre-reinforced polymer. *Struct. Infrastruct. Eng.* **2019**, *15*, 1392–1403. [\[CrossRef\]](#)
26. Qiu, Y.; Zhou, C. Analytical model of large-scale circular concrete columns confined by pre-stressed carbon fibre reinforced polymer composites under axial compression. *Struct. Infrastruct. Eng.* **2021**, *17*, 1062–1075. [\[CrossRef\]](#)
27. Shehata, I.A.; Carneiro, L.A.; Shehata, L.C. Strength of short concrete columns confined with CFRP sheets. *Mater. Struct.* **2020**, *35*, 50–58. [\[CrossRef\]](#)
28. Lam, L.; Teng, J.G. Design-oriented stress-strain model for FRP-confined concrete in rectangular columns. *J. Reinf. Plast. Compos.* **2003**, *22*, 1149–1186. [\[CrossRef\]](#)
29. Jiang, J.; Li, P.; Nistico, N. Local and global prediction on stress-strain behavior of FRP-confined square concrete sections. *Compos. Struct.* **2019**, *226*, 111205. [\[CrossRef\]](#)

30. Shan, B.; Gui, F.C.; Monti, G.; Xiao, Y. Effectiveness of CFRP confinement and compressive strength of square concrete columns. *J. Compos. Constr.* **2019**, *23*, 04019043. [[CrossRef](#)]
31. Boyd, A.J. Rehabilitation of Reinforced Concrete Beams with Sprayed Glass Fiber Reinforced Polymers. Ph.D. Thesis, University of British Columbia, Vancouver, BC, Canada, 2000.
32. Hussain, Q.; Pimanmas, A. Shear strengthening of RC deep beams with openings using sprayed glass fiber reinforced polymer composites (SGFRP): Part 1. experimental study. *KSCE J. Civ. Eng.* **2015**, *19*, 2121–2133. [[CrossRef](#)]
33. Hussain, Q.; Pimanmas, A. Shear strengthening of RC deep beams with sprayed fibre-reinforced polymer composites (SFRP) and anchoring systems: Part 1. Experimental study. *Eur. J. Environ. Civ. Eng.* **2016**, *20*, 79–107. [[CrossRef](#)]
34. Hussain, Q.; Rattanapitikon, W.; Pimanmas, A. Axial load behavior of circular and square concrete columns confined with sprayed fiber-reinforced polymer composites. *Polym. Compos.* **2016**, *37*, 2557–2567. [[CrossRef](#)]
35. Wei, Y.Y.; Wu, Y.F. Unified stress–strain model of concrete for FRP-confined columns. *Constr. Build. Mater.* **2012**, *26*, 381–392. [[CrossRef](#)]
36. Sen, T.; Reddy, H.J. Efficacy of bio derived jute FRP composite based technique for shear strength retrofitting of reinforced concrete beams and its comparative analysis with carbon and glass FRP shear retrofitting schemes. *Sustain. Cities Soc.* **2014**, *13*, 105–124. [[CrossRef](#)]
37. Pimanmas, A.; Hussain, Q.; Panyasirikhunawut, A.; Rattanapitikon, W. Axial strength and deformability of concrete confined with natural fibre-reinforced polymers. *Mag. Concr. Res.* **2019**, *71*, 55–70. [[CrossRef](#)]
38. Sen, T.; Paul, A. Confining concrete with sisal and jute FRP as alternatives for CFRP and GFRP. *Int. J. Sustain. Built Environ.* **2015**, *4*, 248–264. [[CrossRef](#)]
39. Sen, T.; Reddy, H.J. Flexural strengthening of RC beams using natural sisal and artificial carbon and glass fabric reinforced composite system. *Sustain. Cities Soc.* **2014**, *10*, 195–206. [[CrossRef](#)]
40. Rousakis, T.C. Hybrid confinement of concrete by fiber-reinforced polymer sheets and fiber ropes under cyclic axial compressive loading. *J. Compos. Constr.* **2013**, *17*, 732–743. [[CrossRef](#)]
41. Rousakis, T.C. Elastic fiber ropes of ultrahigh-extension capacity in strengthening of concrete through confinement. *J. Mater. Civ. Eng.* **2014**, *26*, 34–44. [[CrossRef](#)]
42. Rousakis, T.C. Reusable and recyclable nonbonded composite tapes and ropes for concrete columns confinement. *Compos. Part B Eng.* **2016**, *103*, 15–22. [[CrossRef](#)]
43. Hussain, Q.; Ruangrassamee, A.; Tangtermsirikul, S.; Joyklad, P. Behavior of concrete confined with epoxy bonded fiber ropes under axial load. *Constr. Build. Mater.* **2020**, *263*, 120093. [[CrossRef](#)]
44. Al-Salloum, Y.A. Influence of edge sharpness on the strength of square concrete columns confined with FRP composite laminates. *Compos. Part B Eng.* **2007**, *38*, 640–650. [[CrossRef](#)]
45. Wang, L.M.; Wu, Y.F. Effect of corner radius on the performance of CFRP-confined square concrete columns: Test. *Eng. Struct.* **2008**, *30*, 493–505. [[CrossRef](#)]
46. Fitzwilliam, J.; Bisby, L.A. Slenderness effects on circular CFRP confined reinforced concrete columns. *J. Compos. Constr.* **2010**, *14*, 280–288. [[CrossRef](#)]
47. Na, L.; Yiyang, L.; Shan, L.; Lan, L. Slenderness effects on concrete-filled steel tube columns confined with CFRP. *J. Construct. Steel Res.* **2018**, *143*, 110–118. [[CrossRef](#)]
48. ASTM A931-08. *Standard Test Method for Tension Testing of Wire Ropes and Strand*; ASTM International: West Conshohocken, PA, USA, 2008.
49. ASTM E8/E8M-13. *Standard Test Methods for Tension Testing of Metallic Materials*; ASTM International: West Conshohocken, PA, USA, 2013.
50. Li, P.; Sui, L.; Xing, F.; Li, M.; Zhou, Y.; Wu, Y.F. Stress–strain relation of FRP-confined predamaged concrete prisms with square sections of different corner radii subjected to monotonic axial compression. *J. Compos. Constr.* **2019**, *23*, 04019001. [[CrossRef](#)]
51. Wang, W.; Sheikh, M.N.; Al-Baali, A.Q.; Hadi, M.N. Compressive behaviour of partially FRP confined concrete: Experimental observations and assessment of the stress-strain models. *Constr. Build. Mater.* **2018**, *192*, 785–797. [[CrossRef](#)]
52. Wang, W.; Sheikh, M.N.; Hadi, M.N. Axial compressive behaviour of concrete confined with polymer grid. *Mater. Struct.* **2016**, *49*, 3893–3908. [[CrossRef](#)]
53. Wang, W.; Wu, C.; Liu, Z.; Si, H. Compressive behavior of ultra-high performance fiber-reinforced concrete (UHPFRC) confined with FRP. *Compos. Struct.* **2018**, *204*, 419–437. [[CrossRef](#)]
54. Saleem, S.; Hussain, Q.; Pimanmas, A. Compressive behavior of PET FRP–confined circular, square, and rectangular concrete columns. *J. Compos. Constr.* **2017**, *21*, 04016097. [[CrossRef](#)]
55. Ozbakkaloglu, T. Behavior of square and rectangular ultra high-strength concrete-filled FRP tubes under axial compression. *Compos. Part B Eng.* **2013**, *54*, 97–111. [[CrossRef](#)]
56. Richart, F.E.; Brandtzaeg, A.; Brown, R.L. *A Study of the Failure of Concrete under Combined Compressive Stresses*; University of Illinois at Urbana Champaign, College of Engineering. Engineering Experiment Station: Champaign, IL, USA, 1928.
57. Benzaid, R.; Mesbah, H.; Chikh, N.E. FRP-confined concrete cylinders: Axial compression experiments and strength model. *J. Reinf. Plast. Compos.* **2010**, *29*, 2469–2488. [[CrossRef](#)]
58. ACI. 440.2 R-02: *Guide for the Design and Construction of Externally Bonded FRP Systems for Strengthening Concrete Structures*; American Concrete Institute: Farmington Hills, MI, USA, 1981.

59. Fardis, M.N.; Khalili, H. Concrete encased in fiberglass-reinforced plastic. *J. Proc.* **2002**, *78*, 440–446.
60. Ilki, A.; Kumbasar, N. Compressive behaviour of carbon fibre composite jacketed concrete with circular and non-circular cross-sections. *J. Earthq. Eng.* **2003**, *7*, 381–406. [[CrossRef](#)]
61. Kumutha, R.; Vaidyanathan, R.; Palanichamy, M.S. Behaviour of reinforced concrete rectangular columns strengthened using GFRP. *Cem. Concr. Compos.* **2007**, *29*, 609–615. [[CrossRef](#)]
62. Lam, L.; Teng, J.G. Strength models for fiber-reinforced plastic-confined concrete. *J. Struct. Eng.* **2002**, *128*, 612–623. [[CrossRef](#)]
63. Mirmiran, A.; Shahawy, M.; Samaan, M.; Echary, H.E.; Mastrapa, J.C.; Pico, O. Effect of column parameters on FRP-confined concrete. *J. Compos. Constr.* **1998**, *2*, 175–185. [[CrossRef](#)]
64. Wu, Y.F.; Wang, L.M. Unified strength model for square and circular concrete columns confined by external jacket. *J. Struct. Eng.* **2009**, *135*, 253–261. [[CrossRef](#)]